



CHORUS

This is the accepted manuscript made available via CHORUS. The article has been published as:

Evidence for excimer photoexcitations in an ordered π -conjugated polymer film

K. Aryanpour, C.-X. Sheng, E. Olejnik, B. Pandit, D. Psiachos, S. Mazumdar, and Z. V. Vardeny

Phys. Rev. B **83**, 155124 — Published 28 April 2011

DOI: [10.1103/PhysRevB.83.155124](https://doi.org/10.1103/PhysRevB.83.155124)

Evidence for Excimer Photoexcitations in an Ordered π -Conjugated Polymer Film

K. Aryanpour,¹ C.-X. Sheng,^{2,3} E. Olejnik,² B. Pandit,² D. Psiachos,¹ S. Mazumdar,^{1,4} and Z. V. Vardeny²

¹*Department of Physics, University of Arizona, Tucson, Arizona 85721, USA*

²*Department of Physics, University of Utah, Salt Lake City, Utah 84112, USA*

³*School of Electronic and Optical Engineering, Nanjing University of Science and Technology, Nanjing, Jiangsu, China 210094*

⁴*College of Optical Sciences, University of Arizona, Tucson, Arizona 85721, USA*

(Dated: March 15, 2011)

We report pressure-dependent transient picosecond and continuous wave photomodulation studies of disordered and ordered films of 2-methoxy-5-(2-ethylhexyloxy) poly(para-phenylenevinylene) (MEH-PPV). Photoinduced absorption (PA) bands in the disordered film exhibit very weak pressure-dependence and are assigned to intrachain excitons and polarons. In contrast, the ordered film exhibits two additional transient PA bands in the mid-infrared that blueshift dramatically with pressure. Based on high-order configuration interaction calculations we ascribe the PA bands in the ordered film to excimers. Our work brings new insight to the exciton binding energy in ordered films versus disordered films and solutions. The reduced exciton binding energy in ordered films is due to new energy states appearing below the continuum band threshold of the single strand.

PACS numbers:

I. INTRODUCTION

Ordered π -conjugated polymer (PCP) films exhibit photophysics remarkably different from dilute solutions or disordered films¹⁻⁴. Explanations given for these differences include photoexcitation branching into intrachain excitons and polarons in the ordered films⁵, as well as formation of a variety of intermolecular species such as polaron-pairs¹⁻³, aggregates^{1,4,6} and excimers⁷⁻¹⁰. Although our understanding of the photophysics due to these interchain species is incomplete, it is generally agreed that the distinctive behavior of the ordered films are due to strong interchain interaction absent in dilute solutions or disordered films. It follows therefore that the ability to vary interchain interactions in a controlled manner should provide an ideal tool for understanding the role of morphology on the photophysics in these materials.

In the present paper we report such a study: we probe pressure effects on the transient picosecond (ps) and continuous wave (cw) photomodulation (PM) spectra of disordered and ordered MEH-PPV films up to 119 kbar. The ordered film exhibits two correlated PA bands absent in the disordered films, which dramatically blue-shift with pressure. We present correlated-electron calculations of excited state absorptions from interacting chains that establish that such blue-shift of PA bands is not expected from aggregates or polaron-pairs. Our calculations establish unambiguously that the primary photoexcited species in ordered MEH-PPV films are excimers, whose PA bands are expected to show pressure-induced blueshift. Specifically, the blueshift indicates pressure-induced changes in the wavefunctions of the initial and final states of these PA bands. We show that such changes in turn indicate nonzero but incomplete intermolecular charge-transfer in the initial state of the excited state absorption, as occurs only in the excimer.

In section II we describe our experimental details and

results. Following this, in sections III and IV we discuss our theoretical approach and computational results. Finally in section V we present our conclusions. Although we are primarily interested in determining the nature of the interchain species in ordered MEH-PPV films, our work also has implications for the exciton binding energy in PCP films. The magnitude of the exciton binding energy in PCPs is a controversial quantity. Our work brings new insight to this subject.

II. EXPERIMENT

We used thin films of polymer samples drop-cast from powder as received from ADS. Transient PM spectroscopy was utilized to resolve the primary photoexcitations. Specifically, we used femtosecond (fs) two-color pump-probe correlation technique with a low-power (energy/pulse ~ 0.1 nJ), high repetition rate (~ 80 MHz) laser system based on a Ti:sapphire (Tsunami, Spectra-Physics) laser having a temporal pulse resolution of 150 fs¹². The pump $\hbar\omega$ was frequency doubled to $\hbar\omega = 3.1$ eV and we used the output beam of an optical parametric oscillator as probe $\hbar\omega$ from 0.24 to 1.1 eV¹². The pump and probe beams were focused on the film surface inside the pressure cell to a spot ~ 100 μm in diameter. The transient PM signal was measured using a phase sensitive lock-in technique at modulation frequency of 30 kHz provided by an acousto-optic modulator. In the mid-IR spectral range we only obtained photoinduced absorption (PA), which is given as the fractional change in transmission $\Delta T/T(t)$. Both T and ΔT were measured using solid state photodetectors, namely Ge, InSb and MCT depending on the spectral range of interest. We carefully aligned the pump and probe beams to reduce the *beam walk* in the experiment. For the steady-state PM spectra we employed a cw laser for pump excitation (Ar+ laser) and an incandescent light (Tungsten Halogen lamp) as a

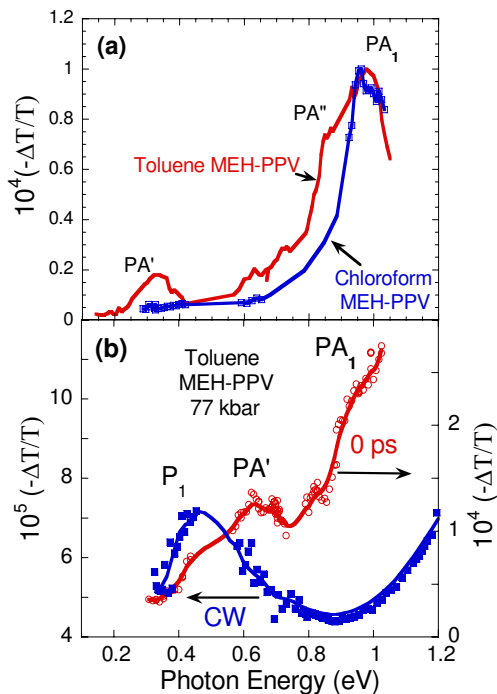


FIG. 1: (Color online) (a) Transient ps PM spectra at $t = 0$ of MEH-PPV(T) (red) and MEH-PPV(C) (blue) films. The exciton PA_1 , and excimer PA' and PA'' bands are assigned. (b) Transient (red) and cw (blue) PM spectra of MEH-PPV(T) at hydrostatic pressure of 77 kbar. PA_1 and PA' are as in (a); P_1 is a polaron band.

probe¹³, using a standard PM set-up based on a $\frac{1}{4}$ met monochromator or FTIR spectrometer. The pump beam intensity was 100 mW/cm² and the probe beam was prefiltered to eliminate excitation above the films optical gap. We used modulation frequency of 350 Hz having peak sensitivity for photoexcitations with about 1 ms lifetime. Solid state detectors such as Si, Ge and InSb spanned the probe photon energy from .25 to 2.2 eV.

Fig. 1a shows the transient PM spectra at time $t = 0$ of two MEH-PPV(T) and MEH-PPV(C) films cast from toluene and chloroform solutions, respectively. Since toluene is a poor solvent for MEH-PPV^{1,4}, MEH-PPV(T) films contain coexisting ordered and disordered phases¹. MEH-PPV(C) contains predominantly the disordered phase^{1,4}. The transient PM of the MEH-PPV(C) contains a single PA band, PA_1 peaked at ~ 0.95 eV, very similar to PA_1 of MEH-PPV in solution, and is correlated to the stimulated emission band in the visible spectral range¹². We therefore identify it as due to intrachain excitons. The MEH-PPV(T) shows two *additional* PA bands, PA' at ~ 0.35 eV and a shoulder PA'' at ~ 0.85 eV. We assign these bands to interchain species.

The band PA' in MEH-PPV was identified previously as due to polarons¹², since the cw polaron band P_1 also peaks at about the same $\hbar\omega(\text{probe}) = 0.4$ eV¹⁴. To confirm the assignment of PA' to interchain species we ap-

plied high hydrostatic pressure P to the MEH-PPV(T) film in a pressure cell. The MEH-PPV film was peeled off the substrate under a microscope, and placed in a diamond-anvil cell equipped with IR-transmitting windows, that was filled with a pressure-transmitting liquid, perfluoro-tri-butylamine to ensure hydrostatic pressure. The pressure inside the cell was measured via the pressure-induced blue-shift in the polymer IR-active C-H frequency at ~ 3000 cm⁻¹, which was pre-calibrated against the pressure-induced change of the well known PL lines of a ruby chip. Fig. 1b shows the transient and cw PM spectra under pressure $P = 77$ kbar. PA' blue-shifts substantially to ~ 0.65 eV, in contrast to the polaron P_1 band in the cw PM spectrum, which does not shift with pressure (Fig. 2b). PA' is therefore not due to polarons.

Fig. 2a shows the MEH-PPV transient PM spectrum for various increasing P -values. PA' and PA'' both grow in intensity relative to PA_1 , and also blue shift together, whereas PA_1 remains at ~ 0.95 eV. The energy shifts of PA_1 , PA' and cw P_1 due to polarons are plotted vs. P up to 120 kbar in Fig. 2b. PA' shifts by about 0.35 eV up to $P = 77$ kbar, and peaks at the same $\hbar\omega(\text{probe})$ at still higher P ; in contrast, P_1 and PA_1 do not shift much with pressure. Fig. 2c shows the decay dynamics of PA' and PA'' at $P = 119$ kbar. The dynamics are clearly identical, coming from the same photoexcitation species.

III. THEORETICAL MODEL AND PARAMETRIZATION

We model the ordered phase as two interacting, cofacially stacked, planar PPV oligomers of equal length^{15,16}. Previously we have shown that high-order configuration interaction (CI) calculations inclusive of all quadruple excitations are essential for finding the PA' band¹⁵. This necessitates the use of the semiempirical π -electron Hamiltonian and also limits the lengths of our oligomers to 3 units. Even with such small system size for the two-chain system our basis size is 1.8 million. For computational simplicity we chose a symmetric arrangement, where each carbon atom of one oligomer lies directly on top of the equivalent carbon atom of the second oligomer. Our calculations are based on the Hamiltonian $H = \sum_{\mu=1,2} H_{\mu} + H_{\mu,\mu'}$, where H_{μ} is the single-chain Pariser-Parr-Pople Hamiltonian¹⁷,

$$H_{\mu} = - \sum_{\langle ij \rangle, \sigma} t_{ij} (c_{\mu,i,\sigma}^{\dagger} c_{\mu,j,\sigma} + H.C.) + \sum_i U n_{\mu,i,\uparrow} n_{\mu,i,\downarrow} + \sum_{i < j} V_{ij} (n_{\mu,i} - 1)(n_{\mu,j} - 1). \quad (1)$$

Here $c_{\mu,i,\sigma}^{\dagger}$ creates a π -electron of spin σ on carbon atom i of the μ th molecule, $n_{i,\mu,\sigma} = c_{\mu,i,\sigma}^{\dagger} c_{\mu,i,\sigma}$ and $n_{\mu,i} = \sum_{\sigma} n_{\mu,i,\sigma}$. We chose the nearest neighbor hopping matrix element $t_{ij} = t = 2.4$ eV for phenyl C-C

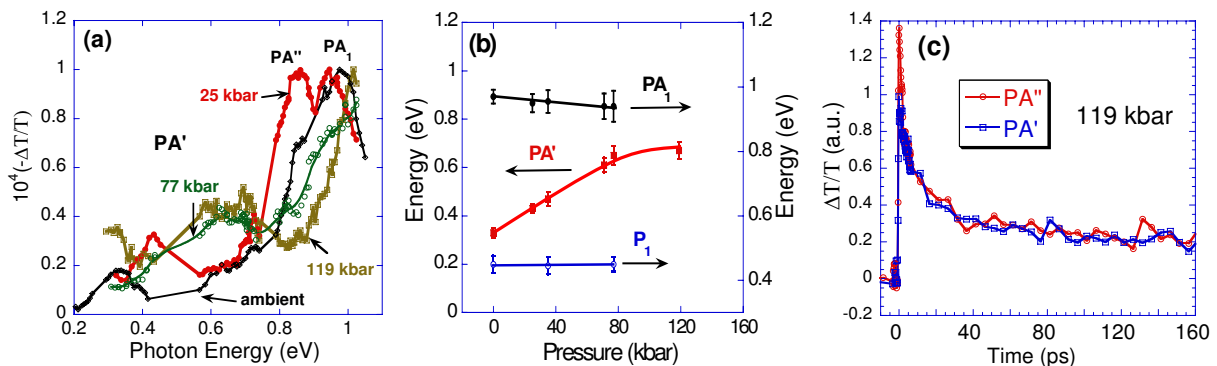


FIG. 2: (Color online) (a) ps transient ($t = 0$) PM spectra of MEH-PPV(T) at ambient pressure, and $P = 25, 77,$ and 119 kbar; the PA bands are assigned as in Fig. 1. (b) Summary of the peak positions for the transient PA' (red) and PA₁ (black) at $t = 0$; and cw P₁ (blue) vs. P . (c) The decay dynamics of the transient PA' and PA'' bands at $P = 119$ kbar.

bonds, and 2.2 (2.6) eV for the intrachain single (double) C-C bonds¹⁸. U is the repulsion between two electrons occupying the same p_z orbital of a C atom, and V_{ij} are intrachain intersite Coulomb interactions parametrized as $V_{i,j} = U/(\kappa\sqrt{1+0.6117R_{ij}^2})$, where R_{ij} is the distance between C atoms i and j in Angstroms. We chose $U = 8.0$ eV and $\kappa = 2^{18}$.

The intermolecular Hamiltonian is written as¹⁵,

$$H_{\mu,\mu'} = - \sum_{(ij),\sigma} t_{ij}^{\perp} (c_{\mu,i,\sigma}^{\dagger} c_{\mu',j,\sigma} + H.C.) + \sum_{i < j} V_{ij}^{\perp} (n_{\mu,i} - 1)(n_{\mu',j} - 1). \quad (2)$$

where $t_{ij}^{\perp} = t^{\perp}$ is restricted to nearest neighbors. For V_{ij}^{\perp} we chose the same functional form as V_{ij} , with a screening parameter $\kappa^{\perp} \leq \kappa$ ¹⁹. We report calculations for $\kappa^{\perp} = \kappa = 2$. Our basis set consists of Hartree-Fock (HF) orbitals localized on individual molecules, allowing calculation of the total charge on the individual oligomers (hereafter ionicity ρ), for each eigenstate.

Both the interaction and the hopping terms in $H_{\mu,\mu'}$ change with pressure. There is no *ab initio* approach to determine these changes. On the other hand, our goal is to understand the effects of enhanced pressure at a qualitative level only, that would allow comparisons between the PA bands expected from the different kinds of intermolecular species. We modeled the effects of increasing pressure by decreasing the intermolecular distance from 0.41 nm at ambient pressure to 0.37 nm at the highest pressures, while increasing t^{\perp} from 0.07 eV to 0.15 eV. Besides reducing intermolecular distances, pressure also causes planarization of individual chains²⁰ which can have two different consequences. First, planarization can increase the effective conjugation length, which in turn will primarily decrease intramolecular transition energies. This is not of interest here, as our focus is on intermolecular interactions. A second consequence of increased planarization is enhanced t^{\perp} , an effect that we

have included.

IV. COMPUTATIONAL RESULTS

The intermolecular species we investigated are: (i) the delocalized covalent ($\rho = 0$) optical exciton $|exc_1\rangle + |exc_2\rangle$, where $|exc_j\rangle$ implies excitation on the j th molecule; (ii) the completely ionic ($\rho = 1$) Coulombically bound polaron-pair, $|P_{\mu}^{+}P_{\mu'}^{-}\rangle$, where P_{μ}^{+} ($P_{\mu'}^{-}$) is a positively (negatively) charged oligomer¹⁻³; and (iii) the excimer or charge-transfer exciton^{7,8,10,15,21}, $|CTX\rangle$,

$$|CTX\rangle = c_c(|exc_1\rangle - |exc_2\rangle) + c_i(|P_1^{+}P_2^{-}\rangle - |P_2^{+}P_1^{-}\rangle) + \dots \quad (3)$$

where \dots denotes higher-order terms; for the $|CTX\rangle$, $0 < \rho < 1$. In all our calculations with the parameters as stated above we have found $|CTX\rangle$ to be the lowest excited state, with the polaron-pair $|P_{\mu}^{+}P_{\mu'}^{-}\rangle$ occurring above the optical exciton.

With completely equivalent PPV oligomers, the polaron-pair is thus never the lowest state at the optical edge and occurs above the optical exciton¹⁵. Since we are interested only in PA from the polaron-pair, which in turn depends only on its wavefunction and not how it is created, we create the polaron-pair by making the PPV oligomers inequivalent. This is done by lowering all HF molecular orbital energies of one oligomer with respect to the other by a fixed energy 2ϵ (in effect creating a heterostructure). For $\epsilon = 0.185$ eV and $\kappa^{\perp} = 1.3$ the lowest excited state of the two-chain system is the polaron-pair with $\rho = 0.9^{19}$.

Fig. 3a shows our calculated PA₁ band of the optical exciton for the two-chain system, as a function of decreasing interchain distance and increasing interactions. Here and in Figs. 3b and c we scaled all excitation energies by the energy E_{1B_u} of the single chain exciton for comparison to experiments. PA₁ exhibits a weak redshift at the highest t^{\perp} , in contrast to the blueshift of the

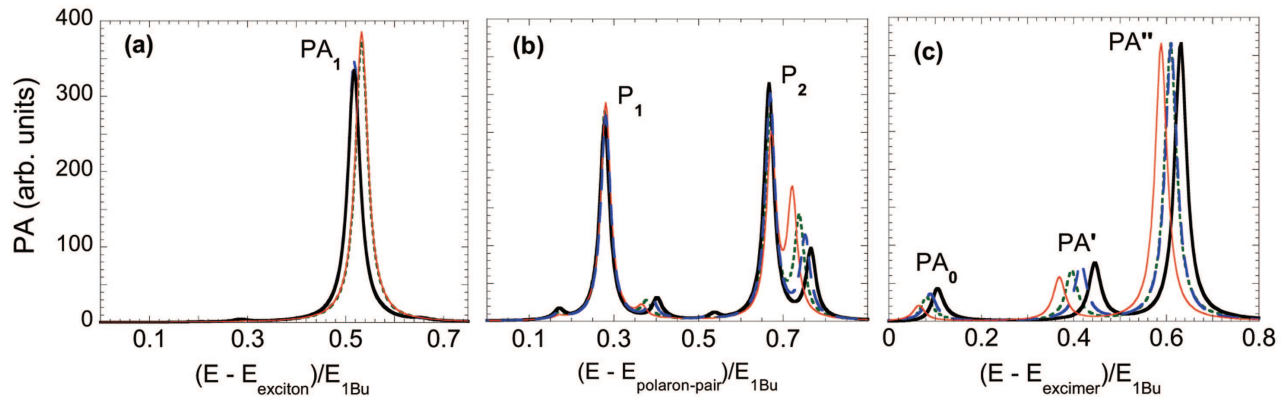


FIG. 3: (Color online) (a) Calculated dependence of PA bands from (a) the two-chain exciton, (b) the polaron-pair, and (c) the excimer, on intermolecular interactions. Red thin curves represent $t^\perp = 0.07$ eV, intermolecular separation $d = 0.41$ nm; green dotted $t^\perp = 0.1$ eV, $d = 0.4$ nm; blue dashed $t^\perp = 0.12$ eV, $d = 0.38$ nm; and black thick $t^\perp = 0.15$ eV, $d = 0.37$ nm.

PA'' band. Our calculated PA bands from the polaron-pair state (see Fig. 3b) are not affected at all by the increased intermolecular interaction. Thus, the PA' and PA'' bands in the ps transient PM spectra of the ordered films cannot be ascribed to excitons or polaron-pairs.

In Fig. 3c we show the calculated PA bands from $|CTX\rangle$, which is the lowest excited state of our Hamiltonian, for several different $H_{\mu,\mu'}$. The lowest energy PA_0 lies outside our experimental spectral range¹⁵, whereas PA' and PA'' are both seen in the experiment. PA' (PA'') originates predominantly from the polaron-pair (exciton) component of $|CTX\rangle$. The pressure-induced blueshifts of the experimental PA' and PA'' energies shown in Fig. 2a are replicated in Fig. 3c. Although quantitative comparisons are difficult, with $E_{1Bu} \sim 2.2$ eV for MEH-PPV the scaled energy shift of the PA' band at the largest $H_{\mu,\mu'}$ is about 0.25 eV, which is close to the maximum measured blueshift of this band shown in Fig. 2a (~ 0.3 eV).

The weak pressure effect on the optical exciton and polaron-pair PA is due to their extreme ionicities, $\rho = 0$ and 1, respectively, that do not change with pressure. In Figs 4a and b we give a mechanistic explanation for the observed blueshifts of the excimer PA bands under pressure. Increased $H_{\mu,\mu'}$ leads to significant decrease in the energy of $|CTX\rangle$ (see Fig. 4a) as a consequence of its increased ionicity (see Fig. 4b). Our calculated ρ for the final state of PA' is considerably larger than ρ for $|CTX\rangle$ (see Fig. 4b), indicating that the PA' absorption, over and above intramolecular polaronlike excitations has also strong contribution from intermolecular charge-transfer excitation. Furthermore, even as the energy of the excimer decreases and its ionicity increases, the energy of the final state of PA' increases (see Fig. 4a) while its ionicity decreases (see Fig. 4b). This indicates that the charge-transfer component of PA' increases with increasing $H_{\mu,\mu'}$ (and hence with increasing pressure). In contrast to the final state of PA' , the final state of PA''

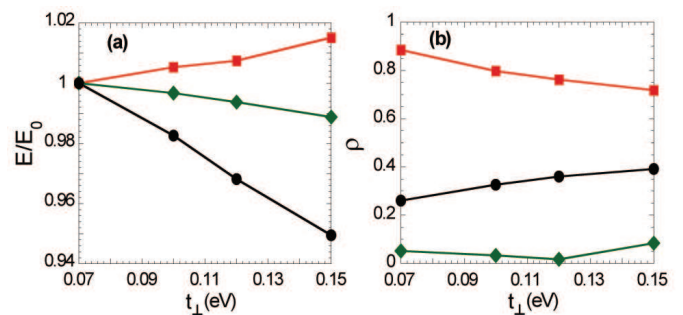


FIG. 4: (Color online) (a) Energies (E) of the excimer (black circles), the final state of PA' (red squares) and the final state of PA'' (green diamonds) as a function of t^\perp , normalized by the energies E_0 of the same states at $t^\perp = 0.07$ eV (ambient pressure). The interchain distances d corresponding to each t^\perp are the same as in Fig. 3. (b) Ionicities of the states in (a).

has a very small ionicity (see Fig. 4b), indicating that PA'' excitation is from the neutral exciton component of $|CTX\rangle$. Hence the increase in PA'' peak energy comes mostly from the decrease in $|CTX\rangle$ energy with P . As seen in Fig. 4a, the energy of the final state of PA'' is nearly independent of t^\perp and actually decreases weakly with increasing t^\perp .

Our analyses in Fig. 3c gives insight to smaller exciton binding energies in ordered films than in solutions of PCPs¹¹. The experimentally measured exciton binding energy is the energy difference between the lowest state with free electron and hole and the bound optical exciton. In solutions and disordered films these states are eigenstates of H_μ alone. The threshold of the continuum band in the single chain, referred to as the nB_u , occurs slightly above a two-photon mA_g exciton in which intrachain charge-separation is much larger than in the optical $1B_u$ exciton (see Fig. 12 in reference 23.) The PA band PA_1 corresponds to the excited state absorp-

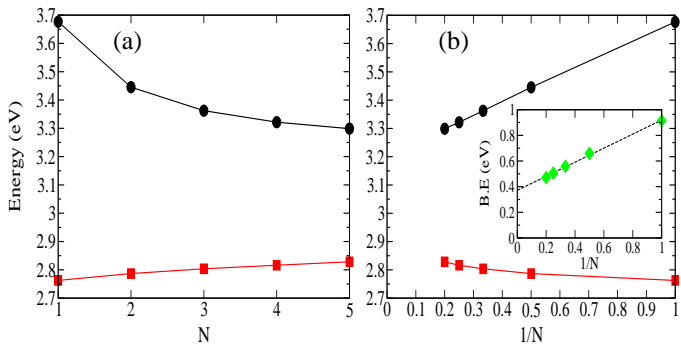


FIG. 5: (Color online) SCI continuum band threshold energy (black circles) and the exciton energy (red squares) versus N and $1/N$ in panels (a) and (b) respectively, where N is the number of interacting 8-unit PPV oligomers. The distance between the chains is 0.4 nm and the interchain hopping $t_{\perp} = 0.1$ eV. The inset (green diamonds) in panel (b) shows the exciton binding energy as a function of $1/N$, with 0.4 eV as the $N \rightarrow \infty$ extrapolated value.

tion from the $1B_u$ to the mA_g , while the nB_u is reached upon further intrachain charge separation²³. In contrast, excited states in ordered films are eigenstates of the *complete* Hamiltonian $H_{\mu} + H_{\mu,\mu'}$. Our wavefunction analysis shows that PA' from the excimer is to a two-photon exciton state with much larger *interchain* charge-transfer than the excimer. The final state of PA' is thus the exact many-chain equivalent of the mA_g in single chains. For interacting chains therefore *interchain charge-separation is energetically less costly*, and it is very likely that further charge-separation is also interchain; hence the observed smaller exciton binding energy in ordered films¹¹ is most probably due to the appearance of new low lying states with greater charge separation below the single-chain continuum, and not because the mA_g or the nB_u comes down in energy due to screening in interacting chains. A complete proof will require quadruples CI calculations of very high energy excited states for multiple (greater than two) chains, which is beyond current computational capability. We present below results of approximate calculations that support this conjecture.

Unlike the even parity two-photon state that is the final state of PA' , the optical exciton as well as the continuum band threshold state are odd parity one-photon states. It is known that they can therefore be determined semiquantitatively from approximate singles-CI (SCI) calculations¹⁸. This remains true independent of the number of chains. The threshold of the continuum band within the SCI is the Hartree-Fock (HF) gap¹⁸. We have calculated the HF gap and the SCI optical exciton energy within our Hamiltonian for 8-unit PPV oligomers, for up to 5 chains. We show these quantities plotted against N in Fig. 5(a), and against $1/N$ in Fig. 5(b), where N is the number of oligomers. The convergence with increasing number of oligomers is obvious from Fig. 5(a) (the small increase in the energy of the optical exciton is expected and is due to nonzero exci-

ton bandwidth, with the optical exciton occurring at the top of the band, as in a H-aggregate¹⁵.) In the inset of Fig. 5(b) we have shown the exciton binding energy versus $1/N$. The $N \rightarrow \infty$ extrapolated exciton binding energy is nearly half of that in the single-chain limit. Importantly, this decrease in exciton binding energy of the many-chain system occurs in spite of PA_1 , which gives the lower limit of the exciton binding energy in the single-chain limit¹⁸, continuing to occur at much higher energy (see Figs. 2(a) and 3(a)). *Thus the reduction in the exciton binding energy is due to the appearance of new states that are absent in the single-chain limit.* Excitonic states derived from the single-chain continue to occur above the many-chain continuum band threshold. We have previously reproduced the observed absorption spectrum of PPV¹⁸ and the energies of the mA_g and the lowest spin triplet nearly quantitatively with our Coulomb parameters²². It is interesting that our extrapolated many-chain exciton binding energy in Fig. 5(b) is very close to the experimental value for PPV films¹¹.

V. CONCLUSIONS

In summary, the significant pressure induced blueshifts exhibited by the transient PA bands in ordered MEH-PPV films indicate *intermediate ionicity for the primary photoexcitation*, *i.e.*, an excimer. PA bands of the optical exciton with ionicity 0, and of the polaron-pair with ionicity nearly 1 are unaffected by pressure. Understanding the role of morphology in the photophysical behavior of PCP films is crucial for their applications in the next generation optoelectronic devices. Our joint theory-experiment work provides a new diagnostic tool for the investigation of the nature of the primary photoexcitations in polymer films, with potentially wide applications in other polymer physics areas.

ACKNOWLEDGMENTS

The Utah group thanks Valentina Morandi and Josh Holt for help with the high pressure and ps measurements. The work at Utah was supported in part by the NSF grant DMR-0803325. The Arizona group thanks Alok Shukla and Zhendong Wang for computational help. The work at Arizona was partially supported by NSF grant DMR-0705163. C.-X.S thanks the support of National Natural Science Foundation of China grant No.61006014.

-
- ¹ L. Rothberg, *Photophysics of Conjugated Polymers, Semiconducting Polymers: Chemistry, Physics and Engineering*, Vol.I, edited by G. Hadziioannou and G. G. Malliaras (John Wiley, 2006), pp. 179-204.
 - ² V. I. Arkhipov, and H. Bassler, *Phys. Stat. Sol. (a)* **201**, 1152 (2004).
 - ³ E. M. Conwell, *Photophysics of conducting polymers, in Organic Electronic Materials: Conjugated Polymers and Low Molecular Weight Solids*, edited by R. Farchioni and G. Grosso (Springer, New York, 2001), pp. 127-180.
 - ⁴ B. J. Schwartz, *Annu. Rev. Phys. Chem.* **54**, 141 (2003).
 - ⁵ P. B. Miranda, D. Moses, and A. J. Heeger, *Phys. Rev. B* **64**, 081201 (2001).
 - ⁶ J. Clark, C. Silva, R. H. Friend and F. C. Spano, *Phys. Rev. Lett.* **98**, 206406 (2007).
 - ⁷ S. A. Jenekhe, and J. A. Osaheni, *Science* **265**, 765 (1994).
 - ⁸ S. Webster, and D. N. Batchelder, *Polymer* **37**, 4961 (1996).
 - ⁹ R. Jakubiak, C. J. Collison, W. C. Wan, and L. J. Rothberg, *J. Phys. Chem. A* **103**, 2394 (1999)
 - ¹⁰ S. Singh, T. Drori and Z. V. Vardeny, *Phys. Rev. B* **77**, 195304 (2008)
 - ¹¹ R. N. Marks, J. J. M. Halls, D. D. C. Bradley, R. H. Friend, and A. B. Holmes, *J. Phys. Condens. Matter* **6**, 1379 (1994). S. Barth and H. Bässler, *Phys. Rev. Lett.* **79**, 4445 (1997).
 - ¹² C.-X. Sheng, M. Tong, and Z. V. Vardeny, *Phys. Rev. B* **75**, 085206 (2007).
 - ¹³ X. M. Jiang, R. Osterbacka, O. Korovyanko, C. P. An, B. Horovitz, R. A. J. Janssen, and Z. V. Vardeny, *Adv. Funct. Materials* **12**, 587 (2002).
 - ¹⁴ T. Drori, E. Gershman, C. X. Sheng, Y. Eichen, Z. V. Vardeny, and E. Ehrenfreund, *Phys. Rev. B* **76**, 033203 (2007).
 - ¹⁵ Z. Wang, S. Mazumdar, and A. Shukla, *Phys. Rev. B* **78**, 235109 (2008). D. Psiachos, and S. Mazumdar, *Phys. Rev. B* **79**, 155106 (2009).
 - ¹⁶ Y.-S. Huang, S. Westenhoff, I. Avilov, P. Sreearunothai, J. M. Hodgkiss, C. Deleener, R. H. Friend, and D. Beljonne, *Nat. Mater.* **7**, 483 (2008).
 - ¹⁷ R. Pariser, and R. G. Parr, *J. Chem. Phys.* **21**, 9865 (1953).
 - ¹⁸ J. A. Pople, *Trans. Faraday Soc.* **49**, 767 (1953).
 - ¹⁹ M. Chandross, S. Mazumdar, M. Liess, P. A. Lane, Z. V. Vardeny, M. Hamaguchi, and K. Yoshino, *Phys. Rev. B*, **55**, 1486 (1997).
 - ²⁰ K. Aryanpour, D. Psiachos, and S. Mazumdar, *Phys. Rev. B* **81**, 085407 (2010).
 - ²¹ J. P. Schmidtke, J. S. Kim, J. Gierschner, C. Silva, and R. H. Friend, *Phys. Rev. Lett.* **99**, 167401 (2007).
 - ²² H. Marciniak, M. Fiebig, M. Huth, S. Schiefer, B. Nickel, F. Selmaier, and S. Lochbrunner, *Phys. Rev. Lett.* **99**, 176402 (2007).
 - ²³ M. Chandross, and S. Mazumdar, *Phys. Rev. B*, **55**, 1497 (1997).
 - ²⁴ M. Chandross, Y. Shimoi, and S. Mazumdar, *Phys. Rev. B* **59**, 4822 (1999)